

# Identification of Three Cysteines as Targets for the $Zn^{2+}$ Blockade of the Human Skeletal Muscle Chloride Channel\*

(Received for publication, February 4 1999)

Lothar L. Kürz<sup>‡</sup>, Holger Klink, Ingrid Jakob, Maya Kuchenbecker, Sandra Benz<sup>§</sup>,  
Frank Lehmann-Horn<sup>§</sup>, and Reinhardt Rüdel

From the Departments of General and <sup>§</sup>Applied Physiology, University of Ulm, D-89069 Ulm, Germany

**Currents through the human skeletal muscle chloride channel hCIC-1 can be blocked by external application of 1 mM  $Zn^{2+}$  or the histidine-reactive compound diethyl pyrocarbonate (DEPC). The current block by  $Zn^{2+}$  strongly depends on the external pH ( $pK_a$  near 6.9), whereas the block by DEPC is rather independent of the pH in the range of 5.5 to 8.5. To identify the target sites of these reagents, we constructed a total of twelve cysteine- and/or histidine-replacement mutants, transfected tsA201 cells with them, and investigated the resulting whole-cell chloride currents. The majority of the mutants exhibited a similar sensitivity toward  $Zn^{2+}$  or DEPC as wild type (WT) channels. Block by 1 mM  $Zn^{2+}$  was nearly absent only with the mutant C546A. Four mutants (C242A, C254A, H180A, and H451A) were slightly less sensitive to  $Zn^{2+}$  than WT. Tests with double, triple, and quadruple mutants yielded that, in addition to C546, C242 and C254 are also most likely participating in  $Zn^{2+}$ -binding.**

The main chloride channel of human skeletal muscle, hCIC-1,<sup>1</sup> is a member of the CIC chloride channel family that is unrelated to any other known ion channels (1). The first membrane topology model of CIC proteins was derived from hydrophathy analysis (2); several times it had to be revised on the grounds of firmer experimental evidence (3–5). Certain mutations in the human CIC-1 gene (reviewed in Ref. 6) lead to myotonia, a disease characterized by muscle stiffness. The study of such myotonia-causing mutations provided first insights into the relationships between the primary sequence and the functions of this channel (7–10). Strong evidence suggests regions between transmembrane segments D3 and the end of D5 to participate in the pore-forming structure (11). However, these results are not in agreement with the most recently postulated topology model of CIC-1 (5). Furthermore, studies of CIC-0 (reviewed in Ref. 1), a homologous chloride channel in the electric organ of *Torpedo*, led to the suggestion of additional protein parts being involved in forming the ion conducting pathway.

CIC channels most likely consist of two subunits (12), and in

the case of CIC-0, each subunit was proposed to contain a single pore (4, 13, 14). Recent evidence speaks against this “double-barreled” channel model, at least in the case of CIC-1 (15).

We have found earlier that the exposure of hCIC-1, stably expressed in HEK-293 cells, to 1 mM  $Zn^{2+}$  leads to a massive reduction of the conducted chloride current (16). The results were compatible with the presence of at least two extracellularly accessible zinc-binding sites and a direct effect on ion permeation, e.g. by obstruction of the pore. The histidyl-reactive diethyl pyrocarbonate (DEPC), applied from the outside, also reduced the currents through hCIC-1. The aim of this study was to identify the target residues for these blockers and, thereby, to draw inferences regarding the membrane topology and the potential location of pore-forming structures. It is known from other proteins, that  $Zn^{2+}$  binding sites are often made up of several and possibly different amino acid side chains (17). Because these residues (histidine, cysteine, or acidic amino acids) can be distant on the primary sequence but close in space, we also hoped that their identification would provide us with the first three-dimensional information on the CIC-1 protein. Therefore, we individually replaced candidate cysteine and histidine residues with alanine, expressed the mutants in tsA201 cells, and characterized their sensitivity toward the blocking agents.

## EXPERIMENTAL PROCEDURES

**Construction and Expression of Mutants**—Site-directed mutagenesis was performed using a polymerase chain reaction-based kit (QuikChange, Stratagene). Mutant constructs contained in the expression vector pRc/CMV were used for transfection of tsA201 cells as described (18). Transient transfection was achieved using the calcium phosphate precipitation method (19) with  $\sim 0.01 \mu\text{g}$  of plasmid DNA per  $3\text{--}5 \times 10^3$  cells/cm<sup>2</sup>. To detect cells expressing recombinant mutant clones after transfection, the tsA201 cells were co-transfected with a plasmid encoding the CD8 antigen and incubated with polystyrene microbeads coated with anti-CD8 antibody (Dynabeads M-450 CD8, Dynal GmbH, Hamburg, Germany) 3 min before electrophysiological characterization.

**Electrophysiology**—Two to three days after transfection, standard whole-cell recordings were performed, using an EPC-7 amplifier (List, Darmstadt, Germany). Only cells to which microbeads had bound were used. For measurements of WT currents, a stably transfected HEK-293 cell line was used (16) or tsA201 cells were transiently transfected as described for the mutants. No differences were observed with these two types of cells regarding electrophysiological characteristics or blocker sensitivity. The standard external solution contained 140 mM NaCl, 4 mM KCl, 2 mM  $CaCl_2$ , 1 mM  $MgCl_2$ , 5 mM HEPES, pH 7.4. For variation of pH, HEPES was substituted on an equimolar basis with MES for pH 5.5–6.7 and with AMPSO for pH 8.0–8.5. The recording pipettes were pulled from borosilicate glass and were heat polished. They had resistances between 1.0 and 2.0 M $\Omega$  when filled with standard internal solution (130 mM CsCl, 2 mM  $MgCl_2$ , 5 mM EGTA, 10 mM HEPES, pH 7.4). More than 60% of the series resistance was compensated for by an analog procedure. Linear leakage or capacitive currents were not subtracted. The currents were filtered using the 3-kHz filter of the amplifier and sampled at various rates. For recording and analysis of experimental data, a combination of three programs (pCLAMP, Axon

\* This work was supported by the Deutsche Forschungsgemeinschaft (Ru 138/20) and the Interdisziplinäres Zentrum für klinische Forschung Ulm. The costs of publication of this article were defrayed in part by the payment of page charges. This article must therefore be hereby marked “advertisement” in accordance with 18 U.S.C. Section 1734 solely to indicate this fact.

<sup>‡</sup> To whom correspondence should be addressed. Tel.: +49 731 503 3617; Fax: +49 731 502 3242; E-mail: lothar.kuerz@medizin.uni-ulm.de.

<sup>1</sup> The abbreviations used are: hCIC-1, chloride channel of human skeletal muscle; DEPC, diethyl pyrocarbonate; WT, wild type; AMPSO, (3-[1, 1-dimethyl-2-hydroxyethyl]amino)-2-hydroxypropane-sulfonic acid; MES, 2-(*N*-morpholino)ethanesulfonic acid.

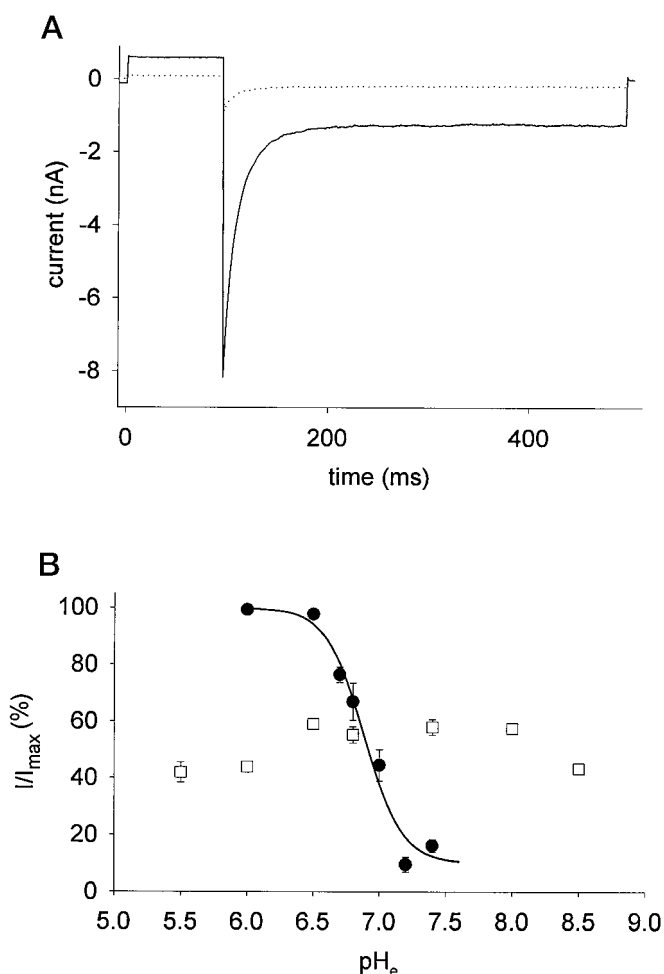


**FIG. 1. Dependence of Zn<sup>2+</sup> and DEPC block on the pH of the external bath solution.** A, examples of chloride current traces recorded in the whole-cell mode from tsA cells expressing WT hClC-1 channels. The control pulse program changed the membrane potential from its holding value of 0 mV first to +50 mV for 100 ms and then to -125 mV for 400 ms and was repeated every 15 s. *Solid line* represents trace obtained in standard bathing solution and *dotted line* after external application of 1 mM Zn<sup>2+</sup>, i.e. at the beginning and end point of blockade. B, current block is expressed as proportion of the amplitudes at +50 mV before ( $I_{max}$ ) and after ( $I$ ) application of blocking agents and plotted against the varied pH of the bathing solution ( $n = 1-6$ ). Shown are fractions obtained in the presence of 1 mM Zn<sup>2+</sup> (●) or in the presence of 1 mM DEPC (□).

Instruments, Foster City, CA; Excel, Microsoft, Unterschleissheim, Germany; SigmaPlot, Jandel Scientific, San Raphael, CA) was used. Differences of current reduction were tested for statistical significance ( $p < 0.05$ ) using one-way analysis of variance followed by the Tukey-Kramer multiple comparisons test (GraphPad InStat, San Diego, CA). All data are shown as mean  $\pm$  S.E.

The pH-dependence as well as concentration dependences of Zn<sup>2+</sup> block were fitted with logistic functions yielding estimates of  $IC_{50}$ ,  $pK_a$ , and Hill coefficients.

To determine the voltage dependence of activation, instantaneous tail current amplitudes at -105 mV were normalized to the extrapolated maximum value and plotted *versus* the test pulse potential, yielding the voltage dependence of the relative open probability,  $P_{open}$  (16). The data were fitted with a single Boltzmann term plus a voltage-independent value:  $I(V) = A \cdot (1 + \exp[(V - V_{0.5})/K_v])^{-1} + \text{constant}$ .

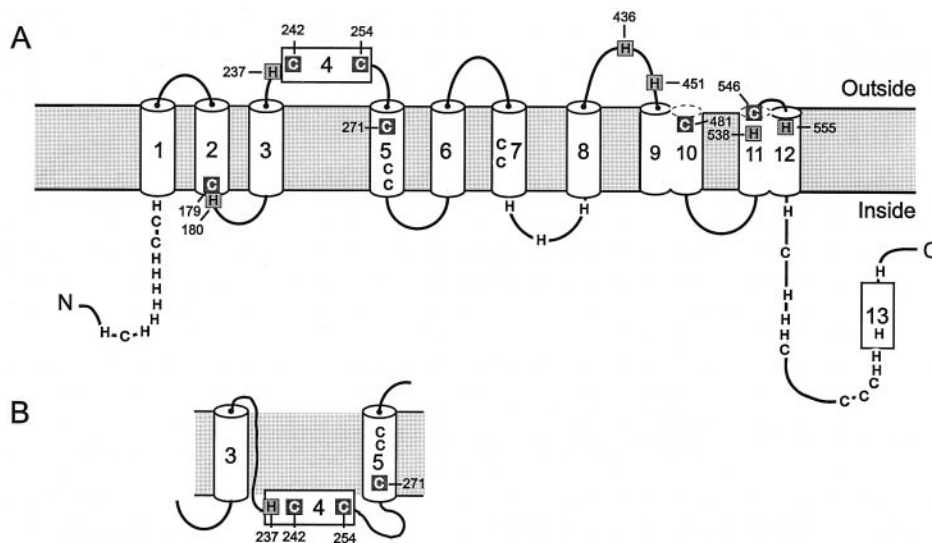
**Application of Reagents—ZnCl<sub>2</sub>** (Sigma Chemical Co., Deisenhofen, Germany) was prepared as a 100 mM stock solution in standard external solution and diluted prior to the experiments. All visible precipitates were eliminated by adding sufficient HCl; no pH change was noted after dilution. DEPC (Fluka, Buchs, Switzerland) was stored desiccated at 4 °C to minimize decomposition by hydrolysis. A 200-mM stock solution in absolute ethanol was freshly prepared every day, kept on ice, and diluted with standard external solution immediately before use. Stock solutions were added to the bath in the appropriate amounts, or else the cells were superfused with the indicated reagent solution. To study the pH dependence, the cells were exposed to bathing solutions of the desired pH, followed by application of the blocking agent.

## RESULTS

**Dependence of Chloride Current Block by Zn<sup>2+</sup> or DEPC on pH**—First we tested the effect of external pH on WT current block by external application of Zn<sup>2+</sup> and DEPC. From the  $pK_a$  and Hill coefficient of such titration curves, we hoped to infer the most likely sort and number of residues participating in the block. Changes of pH alone have profound effects on the gating of hClC-1, whereas outward current amplitudes do not change considerably (20, 21). Block of whole-cell currents was tested by applying repetitive pulses to +50 mV (for maximum channel activation), followed by a hyperpolarizing step at -125 mV to monitor the deactivation time course (Fig. 1A). Block by 1 mM Zn<sup>2+</sup> (registered at +50 mV) showed a strong pH dependence (Fig. 1B). At pH 6.0, the current amplitudes were unaffected, whereas at pH 7.4, the block was almost complete. The apparent  $pK_a$  of the resultant titration curve was 6.9, and the Hill coefficient was 3.0. In contrast, the effect of 1 mM DEPC was practically independent of pH over the range tested, pH 5.5–8.5.

**Functional Characterization of Mutants with Cysteine and Histidine Replaced by Alanine**—According to the topology model of Schmidt-Rose and Jentsch (Ref. 5; see Fig. 2A), the

**FIG. 2. Membrane topology models of hClC-1.** A, model based on results from Schmidt-Rose and Jentsch (5). The positions of all cysteine and histidine residues are indicated by *corresponding letters*, and those of residues mutated in this paper additionally are indicated by *squares* and *numbers*. Segments corresponding to the initially proposed hydrophobic domains D1–D13 (2) are indicated by *numbers*. B, model for D3–D5 region according to Fahlke *et al.* (11).



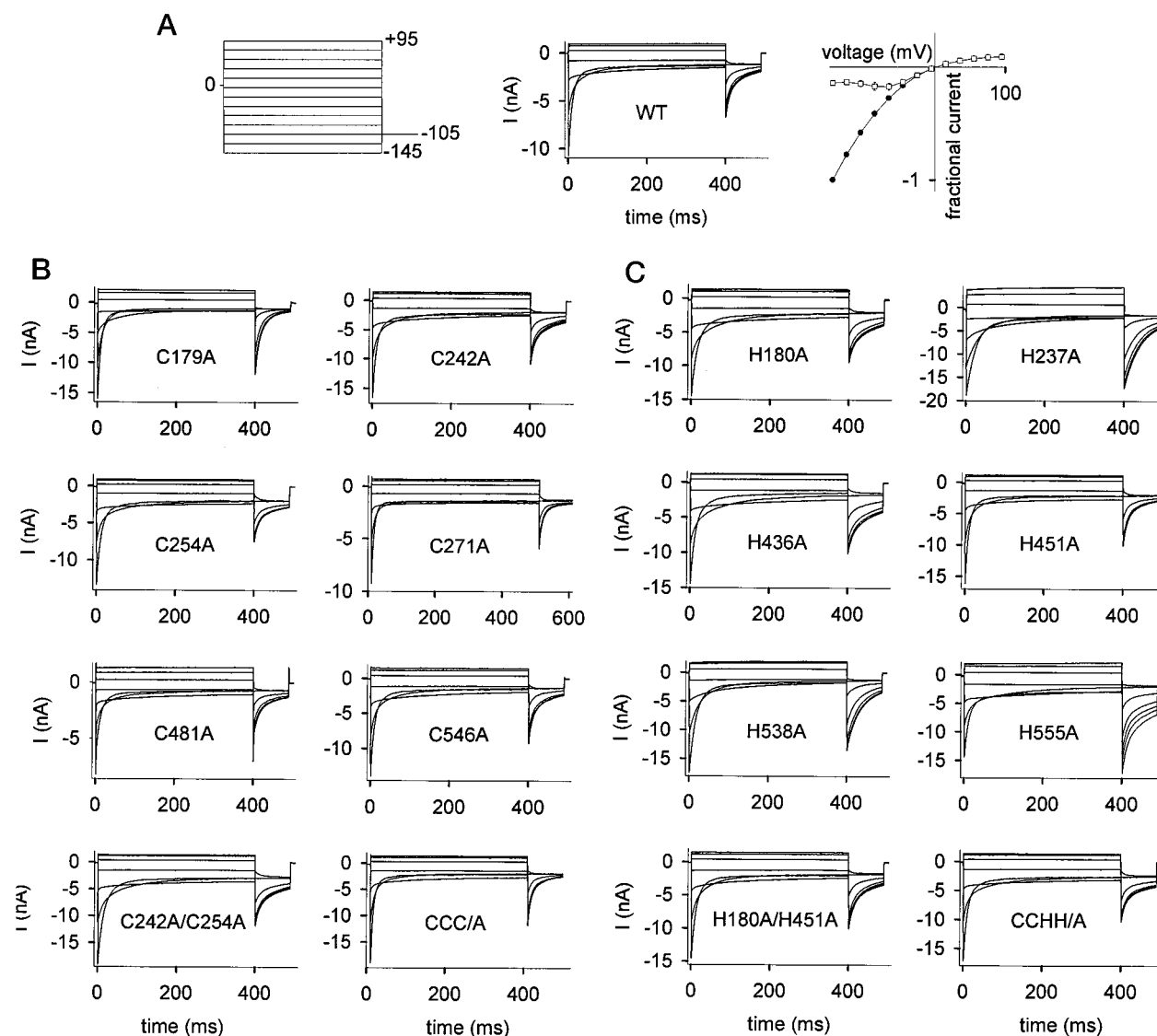


**FIG. 3. Whole cell current recordings from WT as well as from cysteine and histidine mutants.** A, current traces from WT (middle) elicited by the pulse protocol on the left and deduced voltage dependence (right) of normalized instantaneous (circles) and late current (squares) amplitudes, *i.e.* at the beginning and end of the test pulse ( $n = 7$ ). In the middle panel, every second trace has been omitted for clarity. Current traces of all cysteine (B) and histidine (C) mutants analogous to those shown in panel A for WT. Data for constructs C242A/C254A/H180A/H451A (=CCHH/A) are included in panel C; CCC/A = C242A/C254A/C546A. Voltage dependence of instantaneous and late current amplitudes closely resembled that of WT as seen in Fig. 3A, right ( $n = 4-11$ , data not shown).

cysteine residues at positions 242, 254, 271, 481, and 546, and the histidine residues at positions 237, 436, 451, 538, and 555 are potentially accessible from the extracellular environment. To test whether binding of  $Zn^{2+}$  to either of these residues is involved in the observed block, we individually replaced each of these residues by alanine. Positions Cys-179 and His-180 were included in this test because an alternative model placed D2 instead of D4 at the outside (Ref. 4; not shown in figure).

All mutants were functional when expressed in tsA201 cells, and the conducted whole-cell currents were not substantially different from WT currents. They were of similar amplitude and showed the typical deactivation in response to hyperpolarizing pulses as well as inward rectification (Fig. 3).

**Sensitivity of the Cysteine and Histidine Mutants to  $Zn^{2+}$** —In the case of the cysteine mutants C179A, C271A, and C481A, the amount of chloride current block exerted by 1 mM  $Zn^{2+}$  was very similar to that in WT (Fig. 4A). In contrast, block was almost absent with C546A (current reduction only by 17% instead of 83% in WT). Moderate changes (current reduction by 66–67%) were observed in the case of mutants C242A and

C254A. These residues are located in segment D4 (see Fig. 2). The location of this segment is yet unclear, as evidence based on substituted cysteine accessibility suggests it to face (at least in part) the cytoplasm (11), whereas topology studies predict it to be extracellular (5). Furthermore, residues following the C-terminal end of D3 (designated P1) and in D5 have been identified to participate in the pore-forming structure (11).

To test further whether  $Zn^{2+}$  binds to Cys-242 and Cys-254, we constructed a double mutant (C242A/C254A) and investigated its susceptibility to  $Zn^{2+}$  blockade. In standard solutions the electrophysiological characteristics of the double mutant resembled that of WT (Fig. 3B). In the presence of 1 mM  $Zn^{2+}$ , the chloride currents were only decreased by 33% (instead of 83% in WT), confirming the putative capabilities of these two cysteines to bind extracellularly applied  $Zn^{2+}$  and thereby establish channel blockade.

When mutants H436A, H538A, and H555A were in the same way externally exposed to 1 mM  $Zn^{2+}$ , reduction of current was about the same as with WT (Fig. 4B). Currents through the

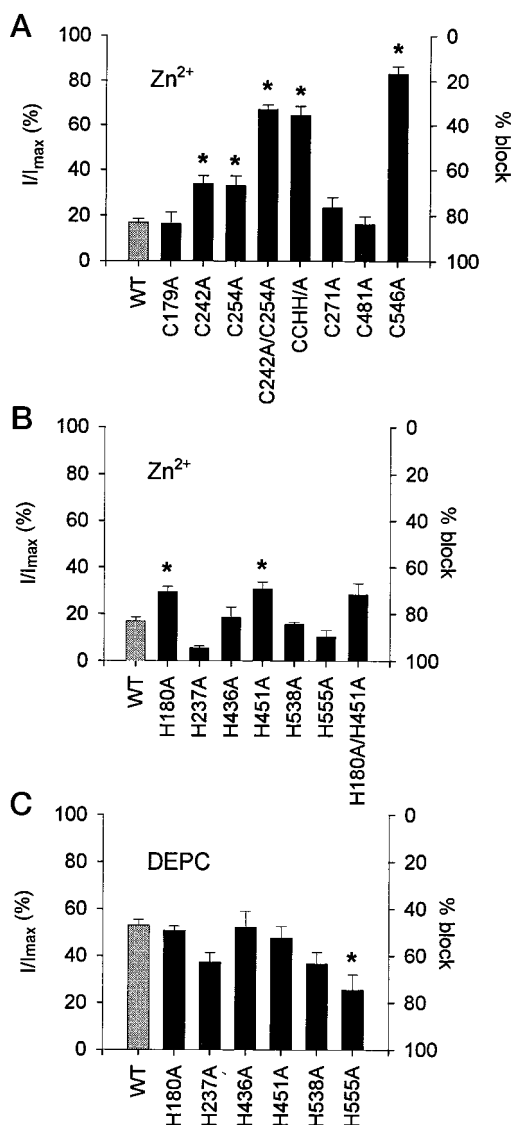


**FIG. 4. Block of chloride current effected by Zn<sup>2+</sup> and DEPC.** For WT and each mutant, the maximum reduction of current is expressed on the left axis in percent of the initial current amplitude at +50 mV ( $\Delta$  100%,  $I = I_{\max}$ , see Fig. 1A;  $n = 3-8$ ). On the right axis, degree of block is plotted (100%  $\Delta$  no current left). Block by 1 mM Zn<sup>2+</sup> for (A) cysteine and (B) histidine mutants. Data for construct C242A/C254A/H180A/H451A (=CCHH/A) are included in panel A. Block of histidine mutants by 1 mM DEPC is shown in panel C. \*, differences statistically significant compared with WT.

mutants H180A and H451A were slightly less blocked by Zn<sup>2+</sup> (statistically significant) and, interestingly, in the case of H237A, Zn<sup>2+</sup> was able to block the chloride currents even by 6% more than in WT. Also, the time course of block was markedly faster in this case (data not shown).

To test for a possible role of His-180 and His-451 in the blocking effect of Zn<sup>2+</sup>, we expressed the mutant H180A/H451A, and additionally C242A/C254A/H180A/H451A, to possibly destroy the binding site completely. The double histidine mutant showed a very similar sensitivity toward Zn<sup>2+</sup> as the two corresponding single mutants (block by ~70%), whereas for the quadruple mutant, it was about as much as with the double mutant C242A/C254A (block by ~33%). This suggests that the two histidine residues are not involved in the blockade exerted by Zn<sup>2+</sup>.

**Concentration Dependence of Zn<sup>2+</sup> Inhibition for Five Cysteine Mutant Constructs**—To further investigate the changes in Zn<sup>2+</sup> block observed for C242A, C254A, and C546A, we meas-

ured current block of these three mutants at different Zn<sup>2+</sup> concentrations. In addition, the double mutant C242A/C254A and the triple mutant C242A/C254A/C546A were also studied. The resulting curves are depicted in Fig. 5. The different degrees of Zn<sup>2+</sup> sensitivity already indicated by the values obtained for 1 mM Zn<sup>2+</sup> was fully confirmed. Whereas for WT, an IC<sub>50</sub> value close to 200  $\mu$ M was obtained, it took ~700–800  $\mu$ M Zn<sup>2+</sup> to produce half-maximal block of the single cysteine mutants C242A and C254A and ~1200  $\mu$ M for the corresponding double mutant. The IC<sub>50</sub> value for C546A was even larger (~1900  $\mu$ M), and after removal of all three cysteines, a value fifty times that of WT was obtained (~9200  $\mu$ M). The Hill coefficient was around 2.6 for WT, and it ranged from 1.6 to 2.5 for the single and double mutants. In the case of the triple mutant, the value was reduced to 0.9.

**Sensitivity of the Histidine Mutants to DEPC**—We also tested the responses of all histidine mutants to extracellularly applied 1 mM DEPC. This reagent preferably modifies histidine residues by covalent binding of the carboxy group to the unprotonated imidazole ring, although modification of other amino acids has been described (22). The chloride currents through H180A, H436A, and H451A were blocked by a similar degree as in cells containing WT channels (47%, Fig. 4C). Block appeared stronger for mutants H237A, H538A, and H555A (63%, 63%, and 74%, respectively), but the difference was significant only for the latter residue.

#### DISCUSSION

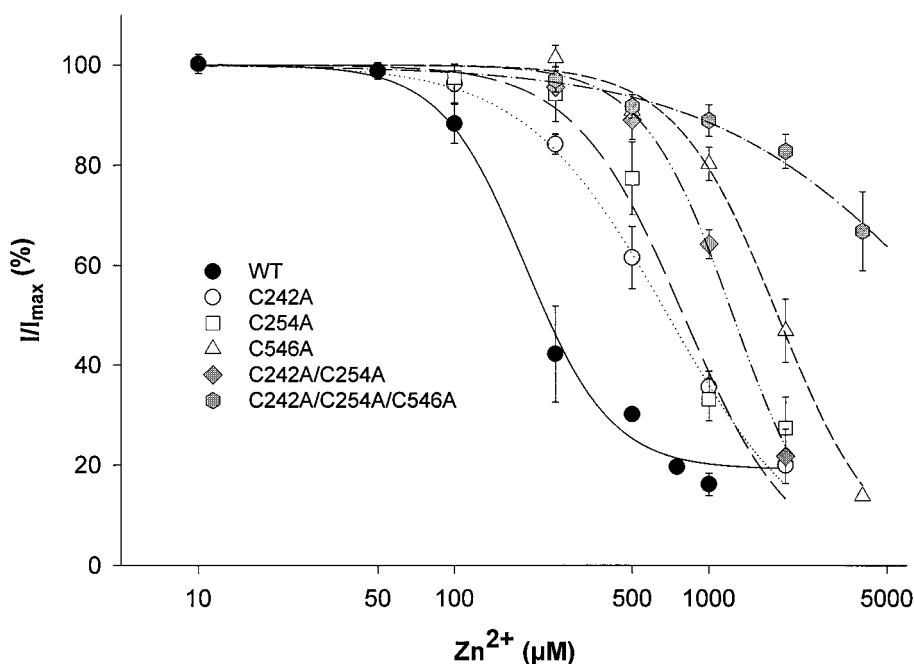
All 14 mutants that we have investigated were functional and showed electrophysiological characteristics resembling those of WT channels. Thus, we can presume that the structural integrity of the channel protein was preserved in each case.

With mutants C242A, C254A, and C546A, the zinc block of the chloride current was smaller than with WT. This suggests that the three cysteines Cys-242, Cys-254, and Cys-546 are involved in the binding of Zn<sup>2+</sup>, creating this effect. This result is surprising in so far as the apparent pK<sub>a</sub> value of the Zn<sup>2+</sup> titration curve (pK<sub>a</sub> = 6.9, Fig. 1B) suggests that a histidine side chain (pK<sub>a</sub> ≈ 6–7) rather than a cysteine (pK<sub>a</sub> ≈ 8–9 in proteins) is the relevant target site. Studies on the pH dependence of CIC-1 current block by Cd<sup>2+</sup>, another group IIb cation with behavior similar to that of Zn<sup>2+</sup>, yielded a pK<sub>a</sub> value of 6.8, *i.e.* nearly identical to ours (23). The authors of that study suggested that histidine residues might be involved. On the other hand, considerable pK<sub>a</sub> shifts of titratable groups are not uncommon in proteins, *e.g.* in our case because of the presence of a positive charge close to the cysteine thiol.

None of the investigated histidine mutants showed a decreased sensitivity toward the histidine-selective reagent DEPC. This could either mean that DEPC has its target site located at a different position or that it exerts its effect by some unspecific mechanism. The apparent lack of pH dependence of the DEPC effect does not allow one to distinguish between these two possibilities.

Because the zinc blockade of WT channels can only be exerted by external application of the metal ion (16), cysteines 242, 254, and 546 must be accessible from the extracellular environment. The finding that the gating parameters were unchanged (16) also led us to assume that Zn<sup>2+</sup> might exert its blockade by a direct effect on chloride permeation, *e.g.* by occlusion of the pore. Thus, the three cysteine residues are presumably located in or near the pore region of the channel. The degree of zinc block was markedly diminished in the case of C546A, and only moderately in the case of the other two mutants. Hence, Cys-546 might be closer to the pore than Cys-242 and Cys-254. The latter two cysteines certainly influence the

FIG. 5. **Concentration dependence of Zn<sup>2+</sup> block.** The fractional current amplitudes recorded at +50 mV at different Zn<sup>2+</sup> concentrations are shown for WT, C242A, C254A, C546A, C242A/C254A, and C242A/C254A/C546A. Lines represent fits with logistic functions ( $n = 1-11$ ).



passage of chloride through the pore when Zn<sup>2+</sup> is bound because the double mutant C242A/C254A is clearly less sensitive toward Zn<sup>2+</sup> as each of the single mutants alone.

Cysteines 242 and 254 are located in the D4 segment, and the residues in and around this region have indeed been postulated to form the channel-lining structure (11). However, when positions 237, 244, 265, and 267 were mutated to cysteines, they were only accessible to internally applied methanethiosulfonate reagents (11). Therefore Fahlke *et al.* (11) suggested D4 to be located at the inside of the membrane (Fig. 2B). In contrast, Schmidt-Rose and Jentsch (5), using glycosylation scanning and protease protection assays, proposed D4 to be located on the extracellular side of the membrane. At first glance, our results seem to speak in favor of the latter model. In addition, the absence of a voltage dependence of the Zn<sup>2+</sup> blockade (16) and the fact that the ClC-1 pore is forming an anion-selective channel lets the possibility of Zn<sup>2+</sup> penetrating this channel seem unlikely. However, positively charged methanethiosulfonate reagents were able to reach cysteine residues within the putative pore (11), and very recent findings imply binding sites for internally applied Cd<sup>2+</sup> at some of these positions (15). Furthermore, work on the GABA receptor, a chloride channel which is also Zn<sup>2+</sup>-sensitive, led to the proposal that Zn<sup>2+</sup> is gaining access to the anion channel lumen, possibly in the form of the complex (ZnCl)<sub>4</sub><sup>2-</sup> (24). The conformation and orientation of the region between D3 and D5 might also be more complex, *e.g.* looping through the membrane, and thereby exposing parts of it to the outside and the inside. Thus, more experimental data are needed to unambiguously assign a certain topology to this area of the protein and to elucidate the pore-lining structure.

Another intriguing observation is that Zn<sup>2+</sup> block of H237A seemed to be stronger (and faster, data not shown) than in the case of WT, although the difference was not statistically significant. The histidine side chain at this position has been proposed to line the channel lumen (11, 15). By substituting it with the smaller, uncharged alanine side chain, the access for Zn<sup>2+</sup> toward its actual target sites (one or more of the three cysteines) nearby might be facilitated. The same argument could explain the somewhat stronger block of mutant H555A by DEPC (Fig. 4C).

The amount of block effected by Zn<sup>2+</sup> in mutants H180A and

H451A is similar to that in mutants C242A and C254A. This led us initially to think of a motif found in some zinc finger proteins: two histidine and two cysteine residues surrounding a Zn<sup>2+</sup> ion in a tetrahedral arrangement (25). After removal of one of the binding partners, Zn<sup>2+</sup> might still be able to bind but with a lower affinity. The lack of any additional blocking influence of the two histidine mutants in the double mutant H180A/H451A and in the construct C242A/C254A/H180A/H451A, however, argues against their potential involvement in Zn<sup>2+</sup> binding.

The mutation producing the largest difference in Zn<sup>2+</sup> sensitivity was C546A. The proposed extracellular accessibility of residue Cys-546 is in agreement with results suggesting that position Leu-549 is also accessible from the exterior (5). Furthermore, ClC-0 mutations situated before and at the end of D12 result in altered permeation properties, implying a possible participation of these regions in forming the channel-lining structure (5, 26).

It is unclear yet whether Cys-242, Cys-254, and Cys-546 participate in the same binding site although the Hill coefficient (3.0) of the titration curve seems suggestive. The substitution of all three residues in the triple mutant C242A/C254A/C546A results in a channel which is almost insensitive to Zn<sup>2+</sup> blockade. The Hill coefficient (~0.9) implies a loss of cooperativity and the removal of one or more binding sites compared with WT (~2.6). In light of the new evidence indicating that ClC-1 has a single pore (15), binding sites made up of corresponding cysteines from both subunits are also plausible.

*Acknowledgments*—We thank M. Arnold, E. Fuchs, and T. Hiller for excellent technical assistance.

#### REFERENCES

- Jentsch, T. J., and Günther, W. (1997) *Bioessays* **19**, 117–126
- Jentsch, T. J., Steinmeyer, K., and Schwarz, G. (1990) *Nature* **348**, 510–514
- Kieferle, S., Fong, P., Bens, M., Vandewalle, A., and Jentsch, T. J. (1994) *Proc. Natl. Acad. Sci. U. S. A.* **91**, 6943–6947
- Middleton, R. E., Pheasant, D. J., and Miller, C. (1994) *Biochemistry* **33**, 13189–13198
- Schmidt-Rose, T., and Jentsch, T. J. (1997) *Proc. Natl. Acad. Sci. U. S. A.* **94**, 7633–7638
- Lehmann-Horn, F., and Rüdell, R. (1996) *Rev. Physiol. Biochem. Pharmacol.* **128**, 195–268
- Fahlke, Ch., Rüdell, R., Mitrovic, N., Zhou, M., and George, A. L., Jr. (1995) *Neuron* **15**, 463–472
- Fahlke, Ch., Beck, C. L., and George, A. L., Jr. (1997) *Proc. Natl. Acad. Sci. U. S. A.* **94**, 2729–2734

9. Pusch, M., Steinmeyer, K., Koch, M. C., and Jentsch, T. J. (1995) *Neuron* **15**, 1455–1463
10. Wollnik, B., Kubisch, C., Steinmeyer, K., and Pusch, M. (1997) *Hum. Mol. Genet.* **6**, 805–811
11. Fahlke, C., Yu, H. T., Beck, C. L., Rhodes, T. H., and George, A. L., Jr. (1997) *Nature* **390**, 529–532
12. Fahlke, Ch., Knittle, T., Gurnett, C. A., Campbell, K. P., and George, A. L., Jr. (1997) *J. Gen. Physiol.* **109**, 93–104
13. Middleton, R. E., Pheasant, D. J., and Miller, C. (1996) *Nature* **383**, 337–340
14. Ludewig, U., Pusch, M., and Jentsch, T. J. (1996) *Nature* **383**, 340–343
15. Fahlke, C., Rhodes, T. H., Desai, R. R., and George, A. L., Jr. (1998) *Nature* **394**, 687–690
16. Kürz, L. L., Wagner, S., George, A. L., Jr., and Rüdell, R. (1997) *Pflügers Arch.* **433**, 357–363
17. Tainer, J. A., Roberts, V. A., and Getzoff, E. D. (1991) *Curr. Opin. Biotechnol.* **2**, 582–591
18. Wagner, S., Deymeier, F., Kürz, L. L., Benz, S., Schleithoff, L., Lehmann-Horn, F., Serdaroglu, P., Özdemir C, and Rüdell, R. (1998) *Muscle Nerve* **21**, 1122–1128
19. Graham, R. L., and van der Eb, A. J. (1973) *Virology* **52**, 456–467
20. Fahlke, Ch., Rosenbohm, A., Mitrovic, N., George, A. L. J., and Rüdell, R. (1996) *Biophys. J.* **71**, 695–706
21. Rychkov, G. Y., Pusch, M., Astill, D. S., Roberts, M. L., Jentsch, T. J., and Bretag, A. H. (1996) *J. Physiol. (Lond.)* **497**, 423–435
22. Miles, E. W. (1977) *Methods Enzymol.* **47**, 431–442
23. Rychkov, G. Y., Astill, D. S., Bennetts, B., Hughes, B. P., Bretag, A. H., and Roberts, M. L. (1997) *J. Physiol. (Lond.)* **501**, 355–362
24. Woollerton, J. R., McDonald, B. J., Moss, S. J., and Smart, T. G. (1997) *J. Physiol. (Lond.)* **505**, 633–640
25. Mackay, J. P., and Crossley, M. (1998) *Trends. Biochem. Sci.* **23**, 1–4
26. Ludewig, U., Jentsch, T. J., and Pusch, M. (1997) *J. Physiol. (Lond.)* **498**, 691–702

## Identification of Three Cysteines as Targets for the Zn<sup>2+</sup> Blockade of the Human Skeletal Muscle Chloride Channel

Lothar L. Kürz, Holger Klink, Ingrid Jakob, Maya Kuchenbecker, Sandra Benz, Frank Lehmann-Horn and Reinhardt Rüdél

*J. Biol. Chem.* 1999, 274:11687-11692.  
doi: 10.1074/jbc.274.17.11687

---

Access the most updated version of this article at <http://www.jbc.org/content/274/17/11687>

### Alerts:

- [When this article is cited](#)
- [When a correction for this article is posted](#)

[Click here](#) to choose from all of JBC's e-mail alerts

This article cites 26 references, 4 of which can be accessed free at <http://www.jbc.org/content/274/17/11687.full.html#ref-list-1>